DOI: 10.13009/EUCASS2019-291

Anomalous Mesh Dependence of Adjoint Solutions Near Walls in Inviscid Flows Past Configurations with Sharp Trailing Edges

Carlos Lozano
Computational Aerodynamics Group
National Institute of Aerospace Technology (INTA)
Carretera de Ajalvir, km. 4. Torrejón de Ardoz, 28850, Spain

Abstract

We show that 2D and 3D inviscid continuous and discrete drag and lift adjoint solutions past sharp trailing edges are generically strongly mesh dependent at and near the wall and do not converge as the mesh is refined. Lift-based adjoint solutions are affected for any flow condition, while drag-based adjoint solutions are affected for transonic lifting flows. This anomalous behavior appears to be linked to the adjoint singularity at the trailing edge.

1. Introduction

Over the past three decades, the adjoint equation approach [1, 2] has been developed to cover a wide variety of CFD-based applications including shape design [3], flow control [4], uncertainty quantification [5] and mesh adaptation [6]. The analysis of the analytic properties of adjoint solutions [7, 8] has uncovered several key features such as the presence of singularities along stagnation streamlines [7] and sharp trailing edges [9]. Both are believed to be singularities of the analytic adjoint solution, but they also feature prominently in numerical solutions, and particularly in adjoint-based mesh adaptation applications [10], as nodes in adjoint-adapted meshes tend to significantly cluster around those areas. In this paper, we describe a related problem first observed in [11] when comparing drag-based adjoint values computed with the Tau code and Nektar++ for transonic, inviscid, steady flow past a NACA0012 airfoil with $M_\infty = 0.8$ and $\alpha = 1.25^\circ$. The same problem was simultaneously found in [12] when performing a mesh convergence study of the same case. The problem is illustrated in Figure 1, where a clear mesh divergence of the adjoint values on the airfoil surface can be observed. This lack of mesh convergence hampers the interpretation of numerical results, making it difficult to compare results obtained with different codes and/or meshes, and can become an issue for mesh adaptation, as the growing size of wall adjoint variables may result in excessive refinement towards the wall (see for example Fig. 7 in [13]). We will show that the problem is not limited to two-dimensional transonic cases or to the drag functional but it is rather a generic problem for inviscid solutions past bodies with sharp trailing edges, which is likely caused by the adjoint singularity at the trailing edge. Likewise, the problem appears in solutions computed with both continuous and discrete adjoint solvers and is, thus, different from other numerical artifacts reported in the literature that plague adjoint solutions (usually from discrete adjoint approaches) due to the lack of dual consistency in the numerical scheme [14, 15, 16]. This distinction is important, as it directly affects what one should expect to see upon refining the mesh. If the adjoint discretization is a consistent approximation to the dual problem (and continuous adjoint discretizations usually are), the method is expected to converge towards the solution of the adjoint PDE with mesh refinement except, of course, at singularities of the adjoint equations. Known singularities include sharp trailing edges and stagnation streamlines and, for transonic flows, the supersonic characteristic that impinges on the root of the shock [13, 17], contact lines [18] such as slip lines/surfaces emanating from sharp trailing edges and the root of the sonic line in transonic solutions (see e.g. Fig. 4 of [7]). Generic points on shocks (barring non-uniqueness problems [19, 20, 21]) and sonic lines [7], on the other hand, seem to be fine, at least for generic cost functions.

DOI: 10.13009/EUCASS2019-291

2. Statement of the problem

2.1 The Adjoint Equations

We begin by recalling a few facts regarding the inviscid adjoint equations. We will focus, for definiteness, on steady, two-dimensional, inviscid flow on a domain Ω with far-field boundary S^∞ and wall boundary S (typically an airfoil profile). The flow is governed by the Euler equations $\nabla \cdot \vec{F} = 0$, where $\vec{F} = (\rho\vec{v}, \rho\vec{v}v_x + p\hat{x}, \rho\vec{v}v_y + p\hat{y}, \rho\vec{v}H)^T$ is the flux vector and $\rho, \vec{v}, p, E, H$ the fluid's density, velocity, pressure, total energy and enthalpy, respectively. The adjoint equations are defined with respect to a functional of the flow variables, or cost function, that we take to be the force exerted by the fluid on the boundary S measured along a direction $\vec{d}$

$$I(S) = \int_S p(\vec{n}_S \cdot \vec{d})dS \tag{1}$$

(where $\vec{n}_S$ is the outward-pointing normal vector to the solid surface). With appropriate choices of $\vec{d}$, eq. (1) can represent the drag or lift on the airfoil.
The corresponding adjoint state $\psi = (\psi_1, \psi_2, \psi_3, \psi_4)^T$ obeys the (adjoint) equation

$$\vec{F}_U{}^T \cdot \nabla\psi = 0 \qquad \text{in } \Omega \tag{2}$$

with the following wall and far-field boundary conditions

$$\begin{aligned} \vec{\varphi} \cdot \vec{n}_S &= \vec{n}_S \cdot \vec{d} \qquad \text{on } S \\ \psi^T(\vec{F}_U \cdot \vec{n}_{S^\infty})\delta U &= 0 \quad \text{on } S^\infty \end{aligned} \tag{3}$$

where $\vec{\varphi} = (\psi_2, \psi_3)$ is the adjoint velocity vector. If the flow solution contains a shock, the above equations need to be modified to account for the appropriate adjoint shock conditions [22, 12]. The adjoint equations (2)-(3) can be discretized for numerical computation (continuous adjoint approach); alternatively, the adjoint system can be derived directly from the discretized flow equations (discrete adjoint approach).

2.2 The singularity at the trailing edge

In [9, 23], Giles and Pierce constructed via conformal mapping a 2D potential adjoint solution that exhibited a singularity at the sharp (cusped) trailing edge of a symmetric Joukowski airfoil, but was otherwise perfectly smooth along the remainder of the wall. A similar solution, with a different cost function, has been explicitly constructed in [24]. The adjoint singularity at the trailing edge has been also observed in solutions computed with the Euler equations [7, 10]. Figure 1 and Figure 2 plot the drag and lift density adjoint variables, respectively, on the surface of a NACA0012 airfoil for inviscid transonic flow with $M_\infty = 0.8$ and $\alpha = 1.25^\circ$ on a set of 6 sequentially refined triangular meshes with up to ~3 million nodes. Each mesh is obtained by uniform refinement of the previous one by splitting in half every mesh edge. When edges are split on the airfoil's surface, the position of the new points is adjusted using cubic splines interpolation such that the new discrete surface follows the original geometry. The computations have been carried out with DLR's discrete adjoint Tau solver [25].

DOI: 10.13009/EUCASS2019-291

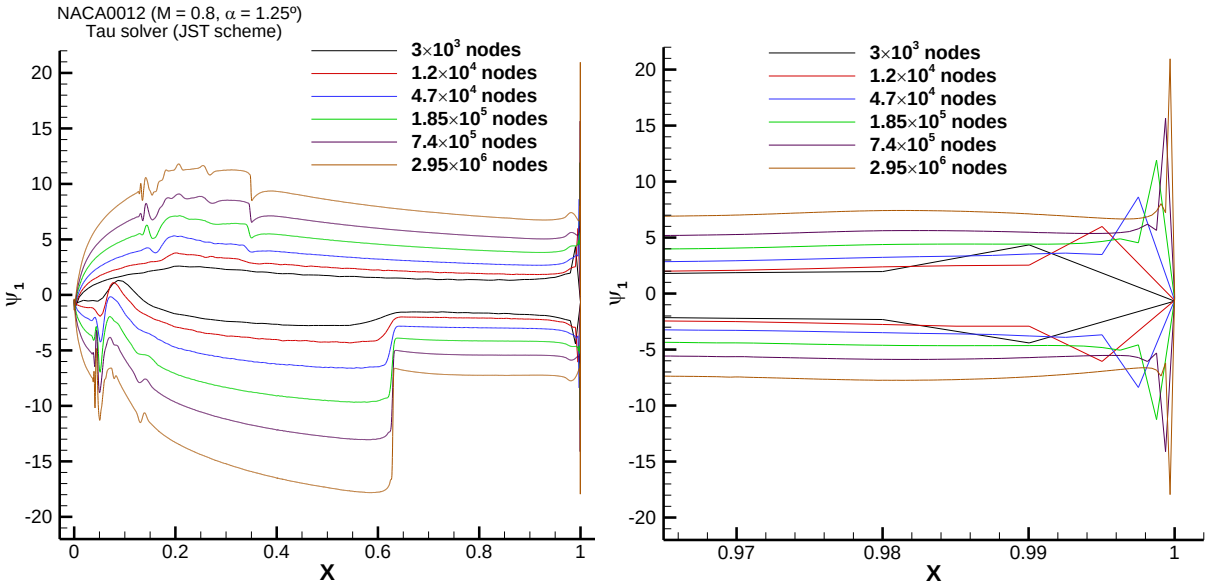

Figure 1: Mesh convergence study of the drag adjoint density solution on a NACA0012 profile (flow conditions $M_\infty = 0.8$ and $\alpha = 1.25^o$)

At the specified conditions, the flow solution has a shock at $x/c \approx 0.63$ on the suction side of the airfoil (with the maximum local Mach number reaching approximately 1.4 on the supersonic side of the shock), and a weaker one on the pressure side. In this case, the actual value of the numerical adjoint solution at the trailing edge is close to zero, but the singularity manifests itself in the large values of the adjoint variable near the trailing edge, which grow continually when the mesh around the trailing edge is refined (Figure 1 and Figure 2 (right)). This mesh dependence should be expected if there is a singularity at the trailing edge: when the mesh is refined, nodes get closer to the singularity and larger and larger values are obtained.

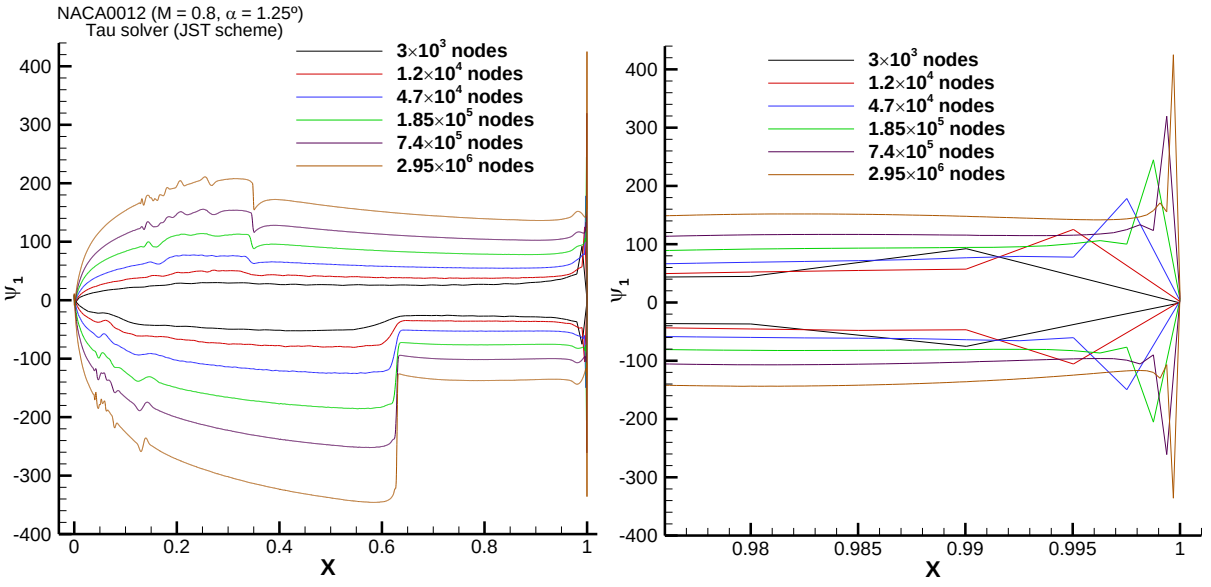

Figure 2: Lift adjoint, NACA0012 ($M_\infty = 0.8$, $\alpha = 1.25^o$)

On the other hand, flow conditions have an effect on the singularity, but this depends on the cost function. Drag adjoint variables are not singular for subcritical flow or zero angle of attack, while lift adjoint variables are singular at any angle of attack and Mach number, as will be shown in the following section. Interestingly enough, the adjoint singularity at the incoming stagnation streamline follows the exact same pattern, although the consequences of this fact for the problem addressed in this paper have not been fully explored.

All of the above is well-known, and simply reflects the sensitivity of the Kutta condition to changes in the geometry of the trailing edge [9]. What is not so well known, and is apparent in Figure 1 and Figure 2, is the very clear

DOI: 10.13009/EUCASS2019-291

mesh divergence of the adjoint solution across the whole airfoil profile, with values growing continually as the mesh is refined. However, adjoint-based sensitivity derivatives are quite accurate [26] and do not reflect a comparable level of mesh dependence.
The observed behavior is not exclusive to the chosen code or numerical settings. Similar trends are observed with Tau's continuous adjoint solver, on different sets of meshes, with different schemes (a second-order central discretization with JST scalar dissipation [27] has been used for Figure 1 and Figure 2, although results with Roe's upwind solver [28] show similar trends). Likewise, the same behavior has been observed with Stanford University's SU2 finite-volume, unstructured continuous adjoint solver [29]. Similarly, [11] reports an offset in absolute value with respect to Tau values of surface drag adjoint values for the transonic NACA case computed with the high-order spectral/hp element solver Nektar++.[1]
In the next section, it will be shown that the issue is strongly related to the trailing edge singularity.

3. Further numerical experiments

We have seen above that, for the NACA0012 airfoil at $M_\infty = 0.8$ and $\alpha = 1.25^\circ$, the adjoint variables on the airfoil profile do not converge as the mesh is refined. Barring bugs or implementation issues, this behavior must have a numerical origin (as argued above, it does not seem to be possible to explain it from the viewpoint of the adjoint p.d.e.) and it is important to know if it is related to the trailing edge singularity and whether it is specific to the flow conditions and cost function chosen. In order to characterize the problem, several test cases have been analyzed with different flow conditions, trailing edge geometries and numerical settings. A 3D case will also be investigated, as well as a 2D viscous (laminar) case.

3.1 2D inviscid flows

A. Symmetric (non-lifting) case

Figure 1 and Figure 2 correspond to a non-symmetric (lifting) transonic case. In a symmetric case, and for the drag-based adjoint, both the singularity and the continuous mesh variation disappear, as can be seen in Figure 3, which shows the drag adjoint solution on a NACA0012 airfoil with $M = 0.8$ and $\alpha = 0^\circ$ on 6 sequentially finer meshes. The solution depicted in Figure 3 does still show a mesh divergence at around $x/c \approx 0.08$ that actually corresponds to the root of the sonic line of the primal flow, which appears to be a singularity of the adjoint solution that can also be spotted in Figure 1, Figure 10 and Figure 14, for example.

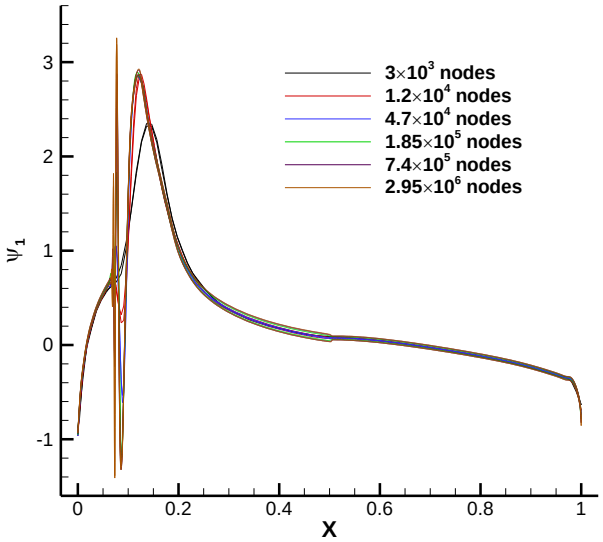

Figure 3: Drag adjoint. NACA0012 ($M_\infty = 0.8$, $\alpha = 0$).

The lift-based adjoint solution, on the other hand, is singular at the trailing edge (and mesh divergent across the entire airfoil profile), as can be seen in Figure 4.

[1] The computed values also show a continuous variation with mesh refinement or order increase (D. Ekelschot, private communication).

DOI: 10.13009/EUCASS2019-291

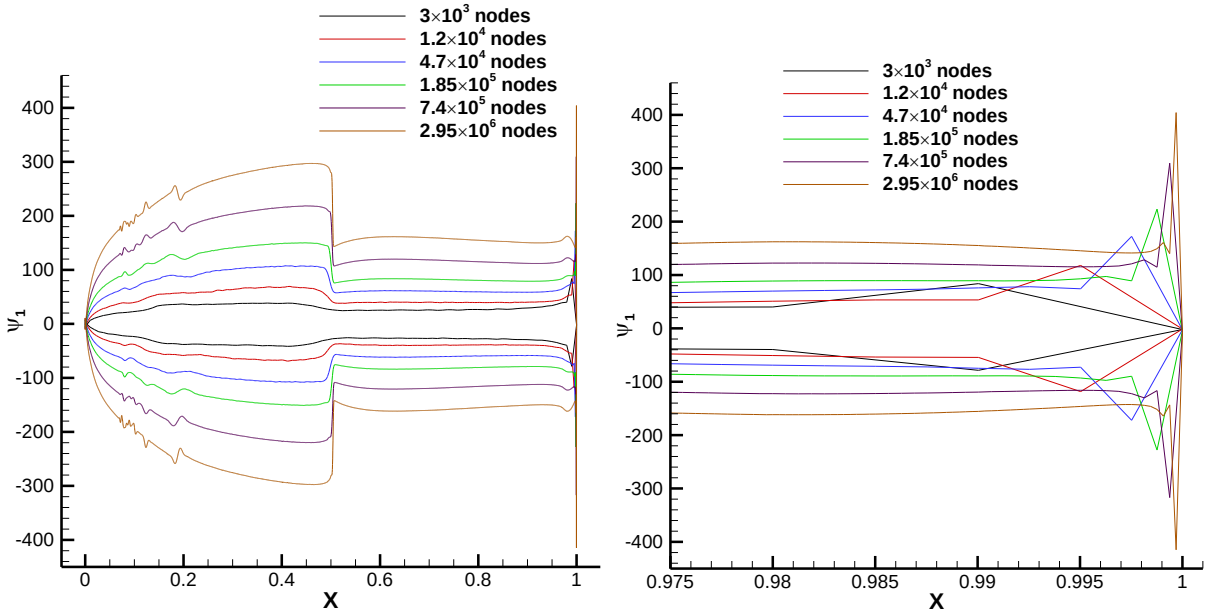

Figure 4: Lift adjoint. NACA0012 ($M_\infty = 0.8$, $\alpha = 0$).

B. Subcritical flow

In a subcritical case, both the trailing edge singularity and the mesh divergence disappear altogether from the drag adjoint solution, even in the lifting case, as can be seen in Figure 5. The lift adjoint solution, on the other hand, is singular at the trailing edge (and mesh divergent) for both symmetric and non-symmetric cases (Figure 6 and Figure 7).

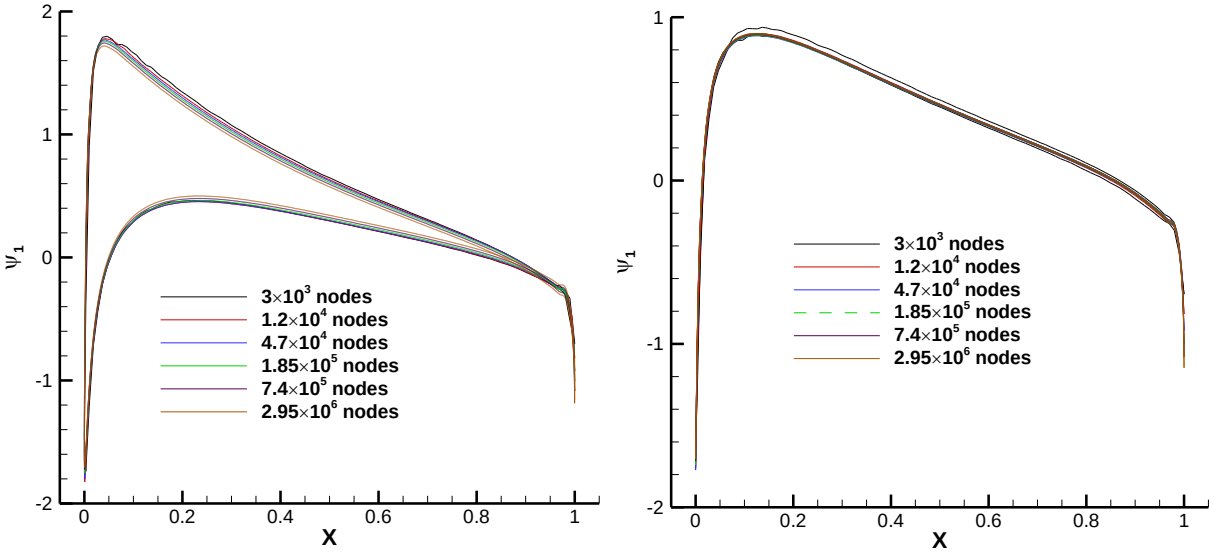

Figure 5: Drag adjoint. NACA0012. Left: $M_\infty = 0.5$, $\alpha = 2^o$. Right: $M_\infty = 0.5$, $\alpha = 0^o$.

DOI: 10.13009/EUCASS2019-291

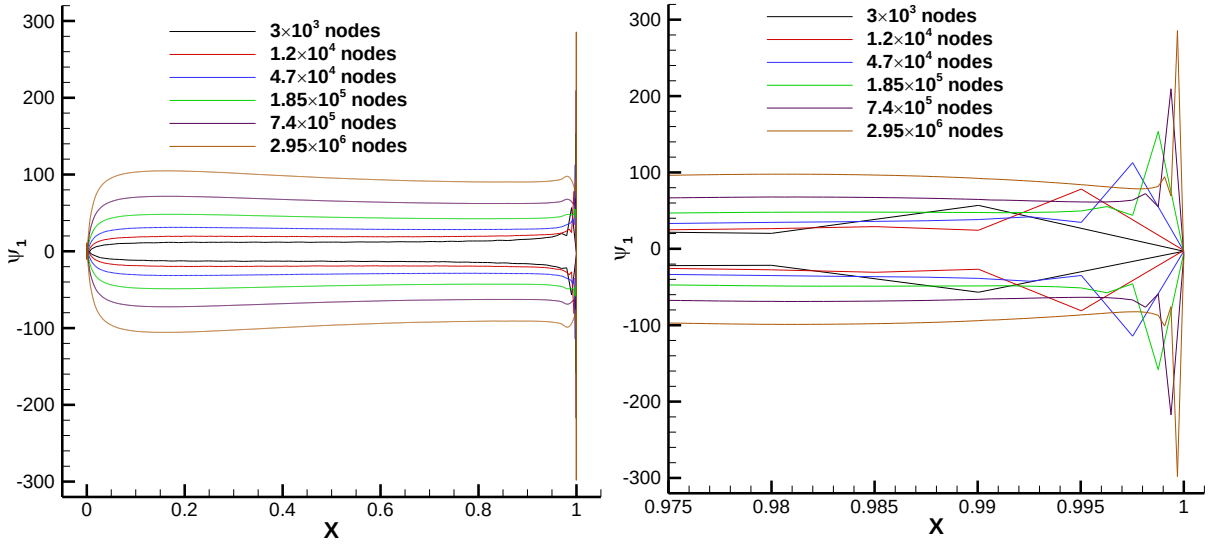

Figure 6**:** Lift adjoint. NACA0012 ($M_\infty = 0.5$, $\alpha = 0^o$).

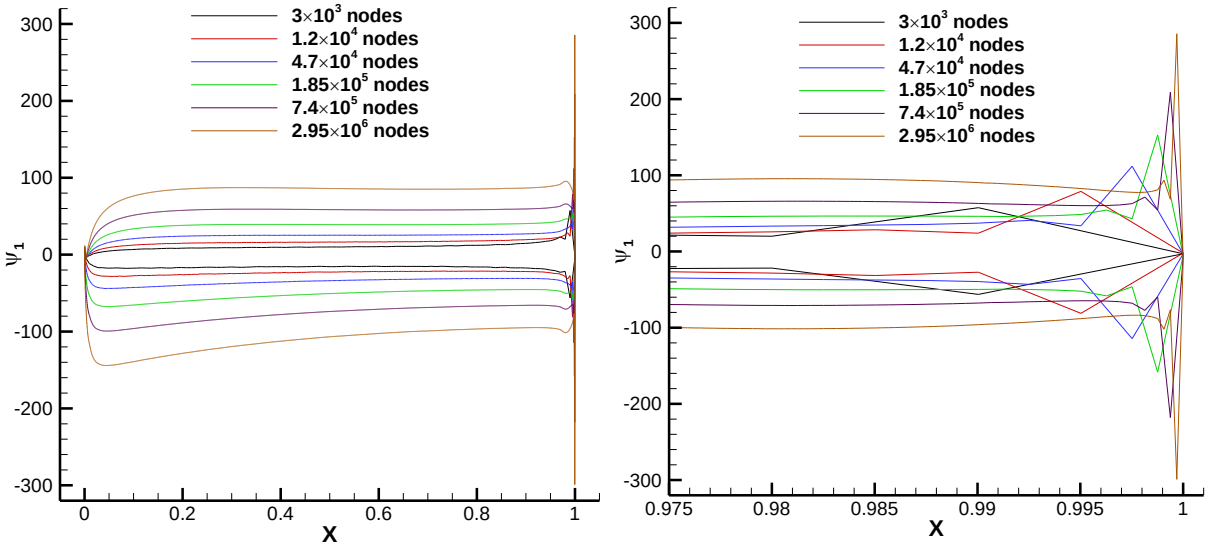

Figure 7: Lift adjoint. NACA0012 ($M_\infty = 0.5$, $\alpha = 2^o$).

C. Modified trailing edge geometry

Several modified NACA0012 airfoils with wedge angles 10.68º and 3.24º (the initial geometry has a wedge angle of about 20.22º), as well as a symmetric Joukowski airfoil and a NACA0012 airfoil with a blunt trailing edge of 0.252% chord are considered. Flow conditions are $M_\infty = 0.8$ and $\alpha = 1.25^o$, and the results of the computations are presented in Figure 8–Figure 11. In all cases, the adjoint singularity is still present, along with a significant level of mesh dependence of the adjoint solutions throughout the airfoil profiles.

DOI: 10.13009/EUCASS2019-291

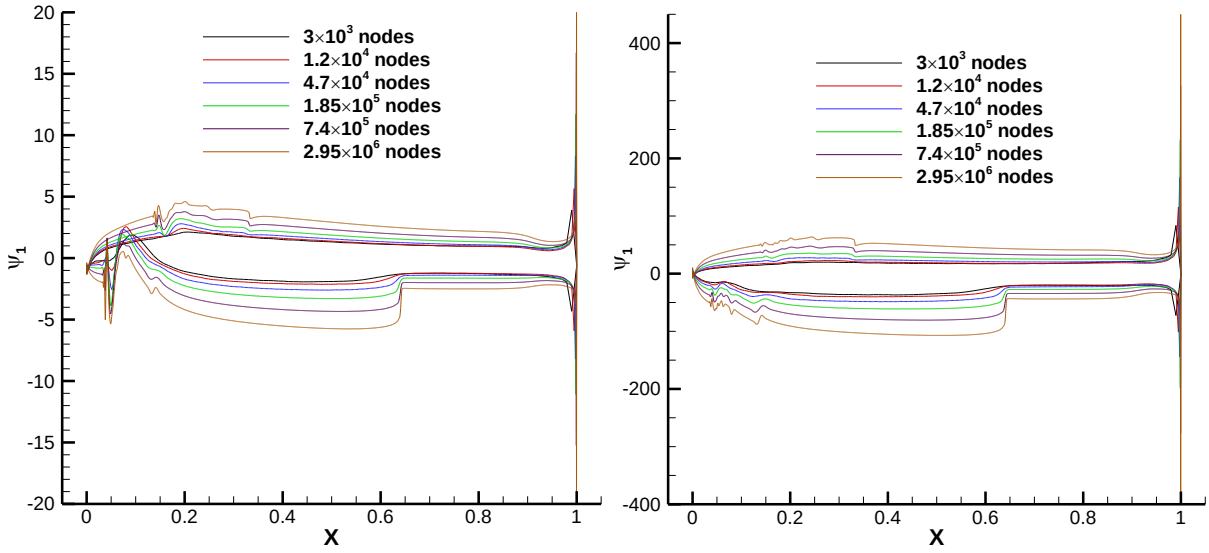

Figure 8: NACA0012 airfoil, wedge angle 10.68º, $M_\infty = 0.8$ and $\alpha = 1.25$. Left: drag adjoint. Right: Lift adjoint.

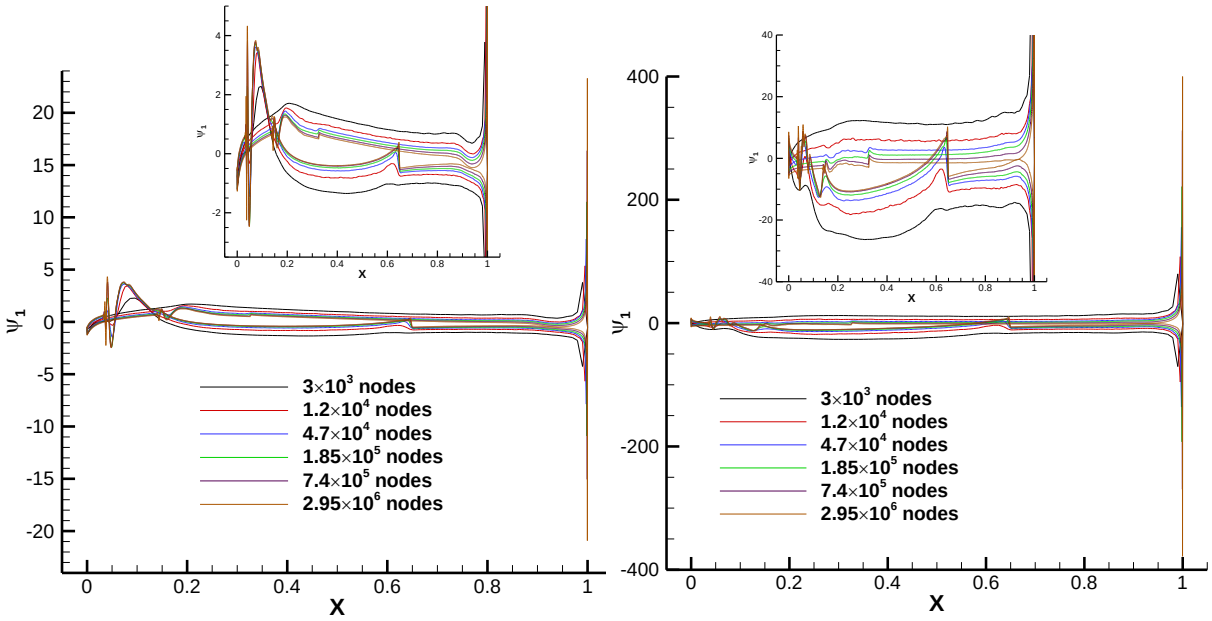

Figure 9: NACA0012 airfoil, wedge angle 3.24º, $M_\infty = 0.8$ and $\alpha = 1.25$. Left: drag adjoint. Right: Lift adjoint.

DOI: 10.13009/EUCASS2019-291

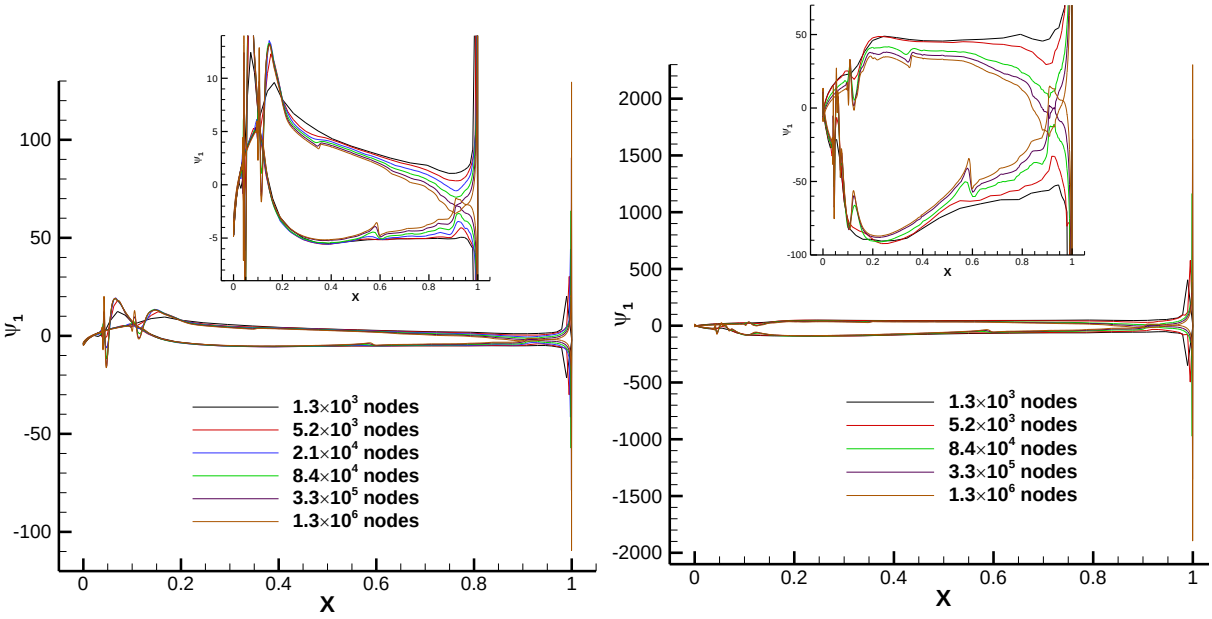

Figure 10: Symmetric Joukowski airfoil, $M_\infty = 0.8$ and $\alpha = 1.25$. Left: drag. Right: Lift adjoint.

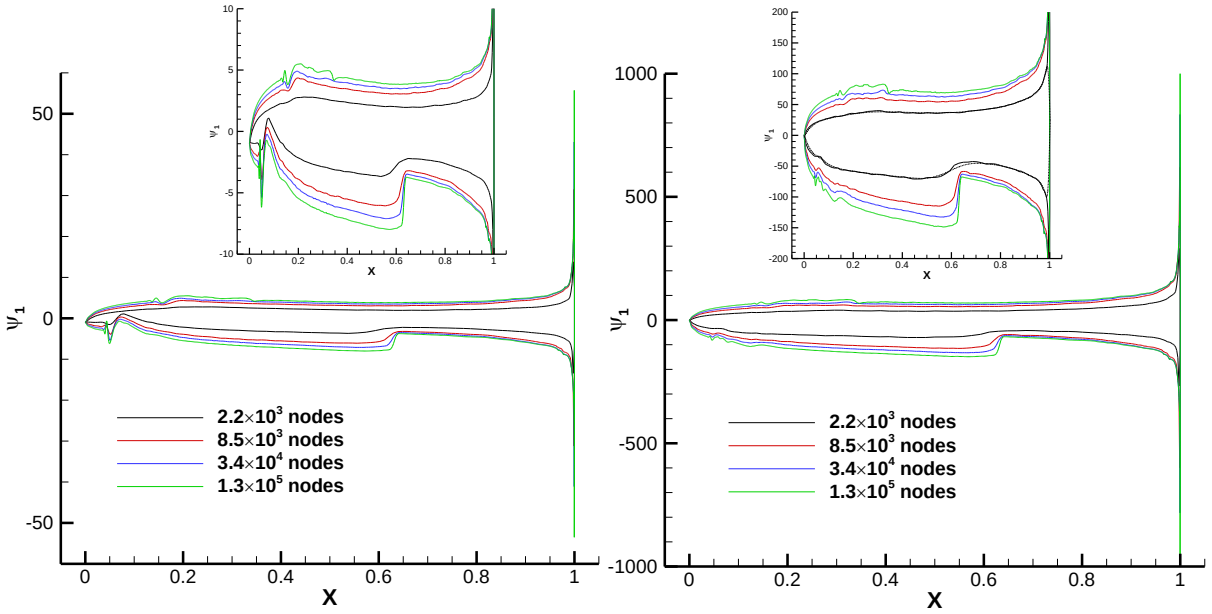

Figure 11: NACA0012 airfoil with blunt trailing edge. $M_\infty = 0.8$ and $\alpha = 1.25$. Left: drag. Right: Lift.

D. Increased dissipation level

Unicity problems of adjoint solutions at primal shocks can be alleviated if the dissipation is increased as the mesh is refined [19]. This can be done easily in schemes such as JST where the dissipation is scaled independently, and we do so in such a way that discontinuities such as shocks are increasingly resolved. Unfortunately, while the overall levels of the adjoint solution on the airfoil are reduced, the trailing edge singularity and the continuous variation with mesh density persist (Figure 12).

DOI: 10.13009/EUCASS2019-291

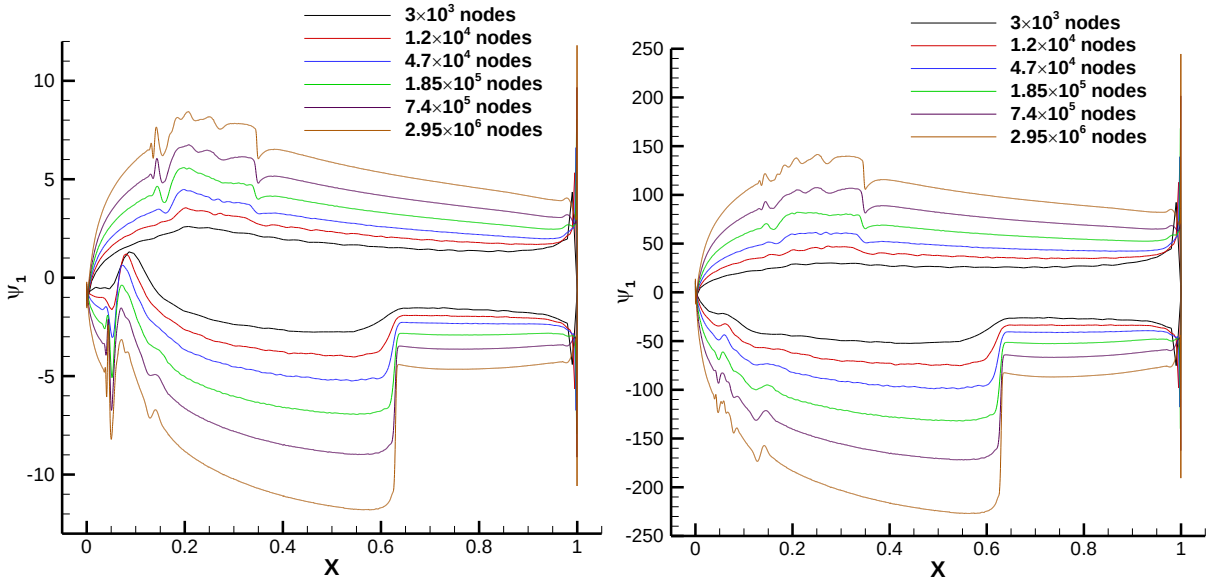

Figure 12: NACA0012 airfoil with $M_\infty = 0.8$ and $\alpha = 0$. JST scheme with dissipation increasing with mesh density. Left: Drag adjoint solution. Right: Lift adjoint solution

Alternatively, we can activate the second dissipation (for both the primal and adjoint solvers) throughout the whole computational domain. This reduces the accuracy of the solution and does not prevent the mesh dependence of the adjoint solution, as can be seen in Figure 13, where results with everywhere active second-order dissipation, both constant and increasing with the mesh density, are shown.

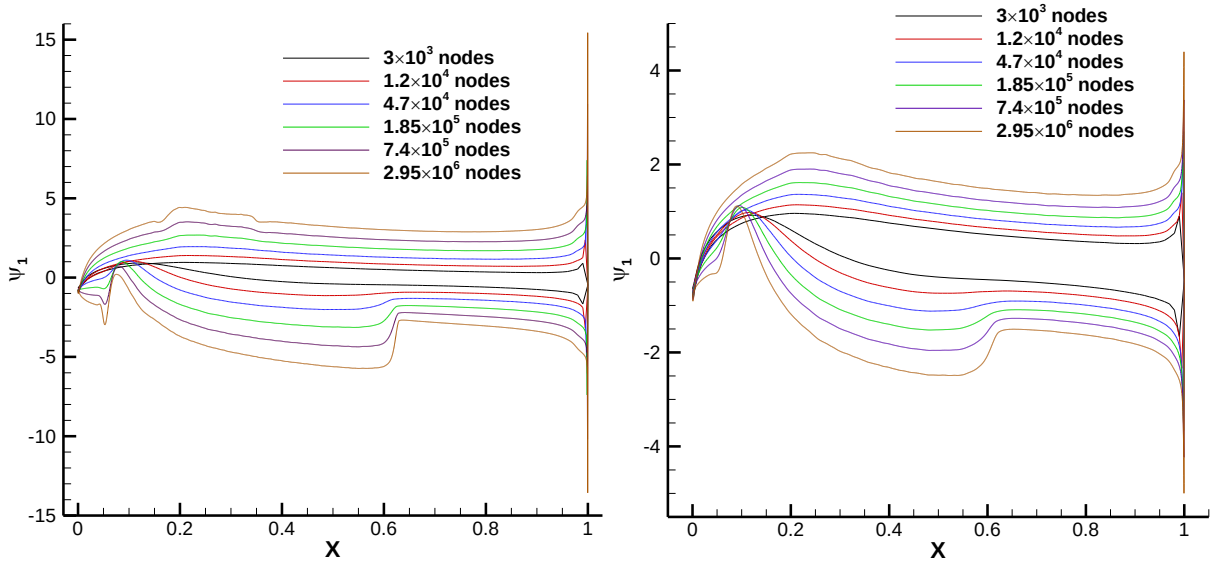

Figure 13: NACA0012 airfoil ($M_\infty = 0.8, \alpha = 0$). Drag adjoint solution. JST scheme with 2nd order dissipation throughout. Left: constant ε_2 . Right: ε_2 increasing with mesh density.

3.2 Inviscid transonic ONERA M6 ($M_\infty = 0.8395$)

Next, a three-dimensional case involving transonic flow past an ONERA M6 wing [30] with $M_\infty = 0.8395$, $\alpha = 0^o$ and $\alpha = 3.06^o$ (and sideslip angle $\beta = 0^o$ in both cases) is considered. At the second flow condition there is a "lambda" shock along the upper surface of the wing. The computations have been carried out with the discrete adjoint Tau solver on four sequentially refined tetrahedral meshes of sizes ranging from 205000 (coarsest) to 105 million elements (finest).

DOI: 10.13009/EUCASS2019-291

Figure 14 shows the drag-based density adjoint distribution at the half-span wing section. We clearly see that, again, in the lifting case the adjoint is singular at the trailing edge, with the accompanying mesh dependence across the entire section, while both the singularity and mesh dependence are absent in the non-lifting case. In the latter case, there is a mesh divergence near the leading edge that actually corresponds to the suction peak and sonic line of the primal flow.

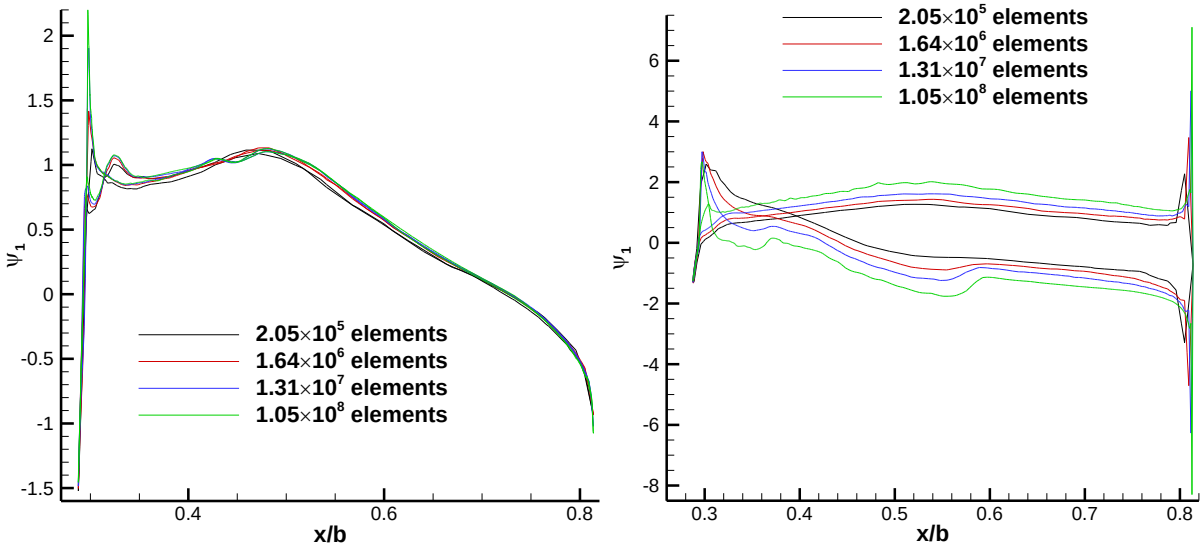

Figure 14: Drag adjoint solution for an ONERA M6 wing with $M_\infty = 0.8395$ and $\alpha = 0^o$ (left) and $\alpha = 3.06^o$ (right).

On the other hand, the lift adjoint solution (Figure 15) is singular at the trailing edge (and not mesh convergent across the whole section) for both flow conditions, as in 2D cases.

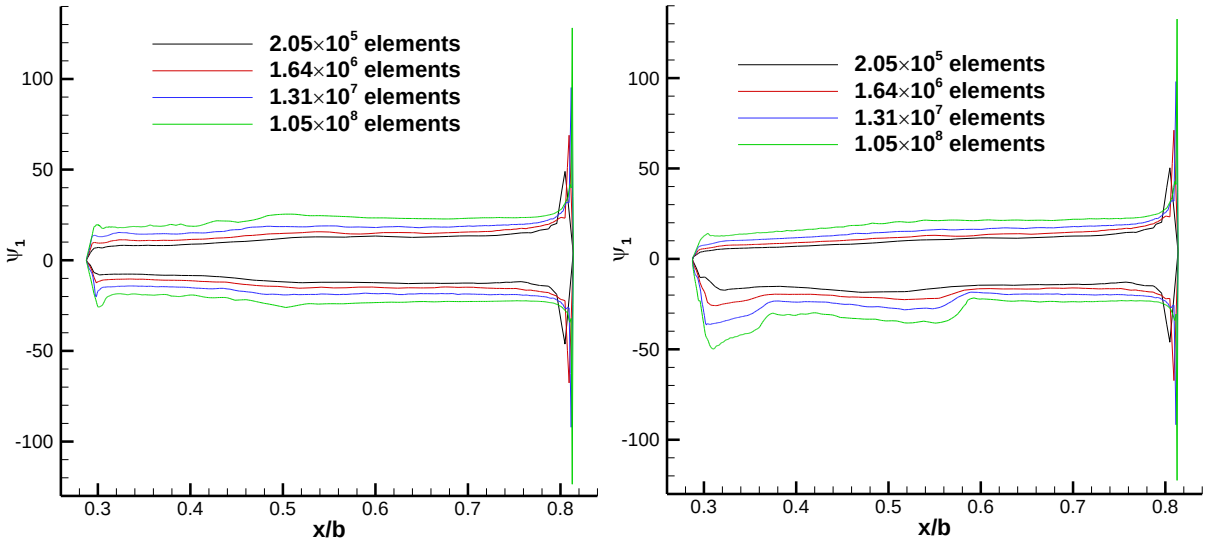

Figure 15: Lift adjoint solution for an ONERA M6 wing with $M_\infty = 0.8395$ and $\alpha = 0^o$ (left) and $\alpha = 3.06^o$ (right).

3.3 Laminar NACA0012 ($M_\infty = 0.5$, $\alpha = 2^o$, $Re = 5000$)

We do not expect to see the above phenomena in viscous flows, as the no-slip condition eliminates the trailing edge singularity. To confirm this idea, we compute the viscous flow past a NACA 0012 airfoil with $M_\infty = 0.5$, $\alpha = 2^o$ and Re = 5000. It is well known that at viscous walls discrete adjoint solutions are typically non-smooth and oscillatory [15] (unless the discretization is dual consistent) and can even have completely arbitrary values decoupled from the interior adjoint [31]. This can interfere with the problem at hand, so we will compute the numerical adjoint solution

DOI: 10.13009/EUCASS2019-291

with Tau's viscous continuous adjoint solver, which was validated (by means of boundary sensitivity derivatives) in [32].

The computations have been performed on a set of sequentially refined hybrid unstructured meshes combining 30 structured layers of quadrilaterals in the boundary layer embedded within a triangular mesh. Wall spacing is $\Delta y_{\min} = 1.35 \times 10^{-4}$ in chord units, and it is kept fixed throughout the experiment, although computations on a mesh with wall spacing half of the above have also been included for completeness. The far-field boundary is approximately 100 chord-lengths away from the airfoil. Adaptation in the structured layer proceeds by edge bisection in the streamwise direction only. Figure 16 shows the results of the computations. Even though there is some degree of mesh dependence, the solutions seem to slowly approach a grid converged solution.

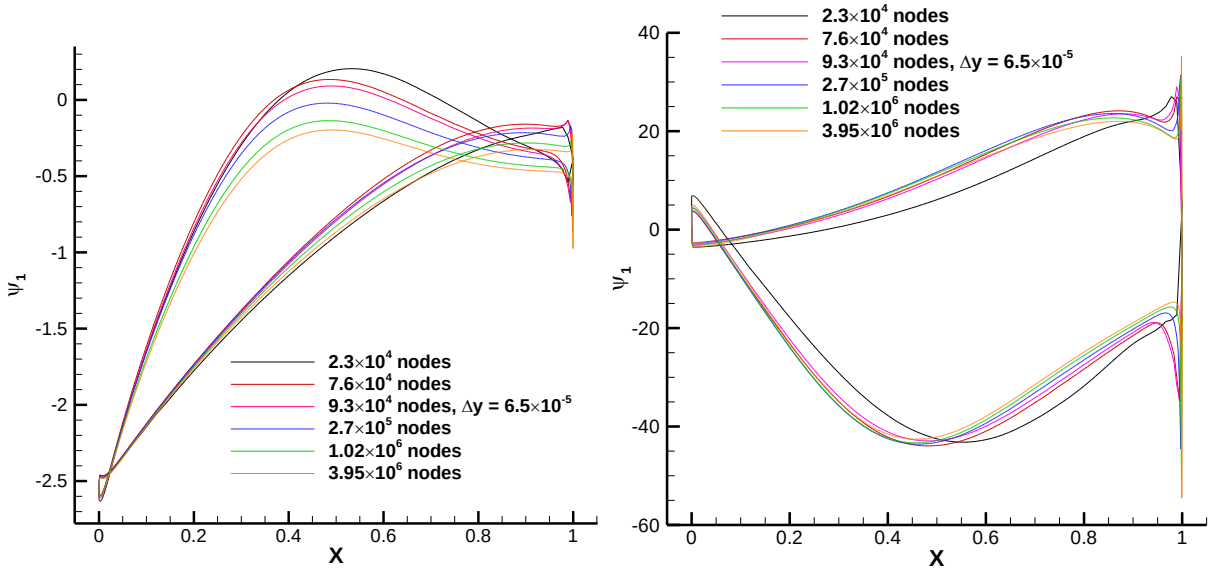

Figure 16: NACA0012 (Re = 5000, $M_\infty = 0.5$, $\alpha = 2^o$). Continuous drag (left) and lift (right) adjoint solutions on the airfoil surface.

3.4 Discussion

The above numerical tests make it clear that the adjoint mesh convergence problem is real and appears to affect inviscid solutions only. While this is of no immediate practical relevance, as adjoint applications focus now on viscous applications, it is still important, from a fundamental viewpoint, to fully understand the behavior of inviscid adjoint solutions for both validation of numerical solvers and a deeper understanding of the adjoint equations. We thus need to find the source of the problem, which has been found to be clearly related to the adjoint singularity at the trailing edge and to affect different cost functions in different ways. Lift adjoint solutions are affected for any flow condition, while drag adjoint solutions seem to be affected only in those cases where the flow conditions result in the formation of a slip line emanating from the trailing edge. There are several possible explanations for this behavior one can come up with.

(1) Singularity of the adjoint p.d.e. or of the solution at solid walls. This seems to be ruled out by the example of the adjoint potential solution, as well as the analysis of the structure of the solutions using the Green function approach [7]. Hence, the origin of the observed behavior must be numerical.

(2) Dual inconsistency of the numerical scheme. I believe that this possibility is ruled out by the fact that the problem is observed in both continuous and discrete adjoint schemes, and in different solvers and with different numerical schemes.

(3) Non-unicity associated to a primal discontinuity. Transonic flow solutions contain singularities such as shocks and, in the lifting case, slip lines/surfaces [33]. At primal shocks, the adjoint equation requires an internal boundary condition which is not enforced numerically and that may lead to wrong adjoint solutions unless sufficient dissipation is applied across the shock [19]. Failing to do so leads to incorrect adjoint values in the shock region that also depend strongly on the mesh density (see chapter 3 in [34], for example). However, the problem we are dealing with also occurs in adjoint solutions for non-shocked flows, and there are shocked (non-lifting) solutions that do not show the

DOI: 10.13009/EUCASS2019-291

problem. Likewise, adding more dissipation does not cure the mesh dependence, so even though the presence of the shock may contribute to the problem, it is certainly not the sole reason.
Regarding the slip line, lift adjoint solutions are singular even without slip lines, so, again, these cannot be the only reason. Furthermore, we have found no trace of singular behavior of the adjoint solutions at the slip line (not even for the drag adjoint in transonic rotational flows). Finally, characteristic curves are parallel to contact discontinuities and slip lines rather than impinging on them, so no adjoint b.c. needs to be imposed, thus closing the door to a possible non-uniqueness mechanism.

(4) Numerical effect triggered by the trailing edge singularity. What all the analyzed cases have in common is the trailing edge adjoint singularity. When the trailing edge is not singular, the adjoint values converge with mesh refinement except at certain singular points. The two phenomena are thus clearly correlated. The issue is whether the established correlation actually implies causation. Adjoint solutions with singularities are well-known, such as in quasi-1D flows, which however do not lead to a comparable level of mesh dependence of the solutions. Two and three-dimensional cases are significantly more complex, and in absence of another plausible mechanism, we are led to believe that the trailing edge singularity (which is already present in the analytic solution) may be responsible for the mesh dependence of adjoint values at the wall. When the mesh is refined, new nodes are placed closer and closer to the trailing edge, resulting in increasingly larger values of the adjoint state. In turn, these large values contaminate the adjoint state across the profile and near wall regions, as only the normal value of the adjoint velocity $\vec{\varphi} = (\psi_2, \psi_3)$ is fixed by the adjoint wall boundary condition (3), triggering the observed mesh divergence.

4. Conclusions

In this paper, we have reported on a problem observed in inviscid adjoint solutions for flows past sharp trailing edges: the lack of mesh convergence of wall and near-wall adjoint values across the entire wall boundary. This lack of mesh convergence properties appears to be a problem of the numerical solution whose details depend on the cost function and the flow conditions. Lift-based adjoint variables are affected at any flow condition, while drag-based adjoint variables are only affected in transonic **lifting** cases.

This problem is not inconsequential: it makes it difficult to interpret and validate numerical results and it can pose a problem in mesh adaptation, as the growing size of wall adjoint variables may result in excessive refinement towards the wall. On the other hand, sensitivity derivatives computed with the singular adjoint solutions are actually quite accurate and do not reflect a comparable level of mesh dependence. This observation may explain why this issue had been largely unnoticed.

What is perhaps more relevant is the fact that the mesh divergence is always associated to a singular behavior at the trailing edge. In those cases where the adjoint is not singular at the trailing edge, the mesh divergence problem is also absent, so the both issues are clearly related. Since the singularity at the trailing edge is inherent in the analytic adjoint solution, we conjecture that the trailing edge singularity is actually causing the mesh divergence.

Acknowledgements

The research described in this paper has been supported by INTA and the Ministry of Defence under the grant Termofluidodinámica (IGB99001). The author wishes to thank J. Ponsin and D. Ekelschot for discussions. The computations reported in the paper were carried out with the TAU Code, developed at DLR's Institute of Aerodynamics and Flow Technology at Göttingen and Braunschweig, which is licensed to INTA through a research and development cooperation agreement. Cross-checking has been also performed with the SU2 code, an open source code developed at the Aerospace Department of Stanford University.

References

[1] A. Jameson. 1988. Aerodynamic Design via Control Theory. J. Sci. Comput. 3(3): 233-260.
[2] A. Jameson. 1995. Optimum Aerodynamic Design Using CFD and Control Theory. AIAA Paper 95–1729.
[3] J. Peter and R. Dwight. 2010. Numerical Sensitivity Analysis for Aerodynamic optimization: A survey of approaches. Comput. Fluids 39(10): 373-391.
[4] B. Munguia, J. Mukhopadhaya and J.J. Alonso. 2019. Active Flow Control Optimization Using the Discrete Adjoint Method. AIAA Scitech 2019 Forum. DOI: 10.2514/6.2019-0695.
[5] G. Allaire. 2015. A review of adjoint methods for sensitivity analysis, uncertainty quantification and optimization in numerical codes. Ingénieurs de l'automobile 836: 33-36.

DOI: 10.13009/EUCASS2019-291

[6] K. Fidkowski and D. Darmofal. 2011. Review of Output-Based Error Estimation and Mesh Adaptation in Computational Fluid Dynamics. AIAA J. 49(4): 673-694.
[7] M. Giles and N. Pierce. 1997. Adjoint Equations in CFD: Duality, Boundary Conditions and Solution Behavior. AIAA Paper 97–1850.
[8] M. Giles and N. Pierce. 2001. Analytic adjoint solutions for the quasi-one-dimensional Euler equations. J. Fluid Mechanics 426: 327-345.
[9] M. Giles and N. Pierce. 2002. Adjoint error correction for integral outputs. In: Error Estimation and Solution Adaptive Discretization in Computational Fluid Dynamics (Lecture Notes in Computer Science and Engineering, vol. 25), T. Barth and H. Deconinck, Eds. Springer Verlag, Berlin. pp. 47-95.
[10] D. Venditti and D. Darmofal. 2002. Grid Adaptation for Functional Outputs: Application to Two-Dimensional Inviscid Flows. J. Comput. Phys. 176: 40–69.
[11] D. Ekelschot. 2016. Mesh adaptation strategies for compressible flows using a high-order spectral/hp element discretisation. Ph.D. Thesis. Department of Aeronautics, Imperial College (London).
[12] C. Lozano. 2018. Singular and Discontinuous Solutions of the Adjoint Euler Equations. AIAA J. 56(11): 4437-4452.
[13] M. Yano and D. Darmofal. 2012. C1.3 Flow over the NACA0012 airfoil, inviscid and viscous, subsonic and transonic. In: 1st International Workshop on High-Order CFD Methods. January 7-8, 2012 at the 50th AIAA Aerospace Sciences Meeting, Nashville, Tennessee.
[14] J. Hicken and D. Zingg. 2014. Dual Consistency and Functional Accuracy: a Finite-difference Perspective. J. Comput. Phys. 256: 161-182.
[15] M. Giles, M. Duta, J.-D. Müller and N. Pierce. 2003. Algorithm Developments for Discrete Adjoint Methods. AIAA J. 41(2): 198-205.
[16] C. Lozano. 2016. A note on the dual consistency of the discrete adjoint quasi-one-dimensional Euler equations with cell-centered and cell-vertex central discretizations. Comput. Fluids 134-135: 51-60.
[17] F. Sartor, C. Mettot and D. Sipp. 2015. Stability, Receptivity, and Sensitivity Analyses of Buffeting Transonic Flow over a Profile. AIAA J. 53(7): 1980-1993.
[18] F. Alauzet and O. Pironneau. 2012. Continuous and discrete adjoints to the Euler equations for fluids. Int. J. Num. Meth. Fluids 70(2): 135-157.
[19] M. Giles. 2003. Discrete adjoint approximations with shocks. In: Hou T.Y., Tadmor E. (eds) Hyperbolic Problems: Theory, Numerics, Applications, pp. 185-194. Springer, Berlin, Heidelberg.
[20] M. Giles and S. Ulbrich. 2010. Convergence of linearized and adjoint approximations for discontinuous solutions of conservation laws. Part 1: linearized approximations and linearized output functionals. SIAM J. Numer. Anal. 48(3): 882-904.
[21] M. Giles and S. Ulbrich. 2010. Convergence of linearized and adjoint approximations for discontinuous solutions of conservation laws. Part 2: adjoint approximations and extensions. SIAM J. Numer. Anal. 48(3): 905-921.
[22] A. Baeza, C. Castro, F. Palacios and E. Zuazua. 2009. 2-D Euler Shape Design on Nonregular Flows Using Adjoint Rankine-Hugoniot Relations. AIAA J. 47(3): 552-562.
[23] M. Giles and N. Pierce. 1999. Improved Lift and Drag Estimates Using Adjoint Euler Equations. AIAA paper 99-3293.
[24] C. Lozano. 2019. Watch Your Adjoints! Lack of Mesh Convergence in Inviscid Adjoint Solutions. AIAA J. (under review).
[25] D. Schwamborn, T. Gerhold and R. Heinrich. 2006. The DLR TAU-Code: Recent Applications in Research and Industry. In: ECCOMAS CFD 2006, European Conference on CFD, Egmond aan Zee, The Netherlands.
[26] C. Lozano. 2017. On Mesh Sensitivities and Boundary Formulas for Discrete Adjoint-based Gradients in Inviscid Aerodynamic Shape Optimization. J. Comput. Phys. 346: 403–436.
[27] A. Jameson, W. Schmidt and E. Turkel. 1981. Numerical Solutions of the Euler Equations by Finite Volume Methods Using Runge-Kutta Time-Stepping Schemes. AIAA Paper 81-1259.
[28] P. Roe. 1981. Approximate Riemann Solvers, Parameter Vectors and Difference Schemes. J. Comput. Phys. 43(2): 357-372.
[29] T. Economon, F. Palacios, S. Copeland, T. Lukaczyk and J.J. Alonso. 2016. SU2: An Open-Source Suite for Multiphysics Simulation and Design. AIAA J. 54(3): 828-846.
[30] V. Schmitt and F. Charpin. 1979. Pressure Distributions on the ONERA-M6-Wing at Transonic Mach Numbers. Experimental Data Base for Computer Program Assessment. Report of the Fluid Dynamics Panel Working Group 04, AGARD AR 138.
[31] W.K. Anderson and V. Venkatakrishnan. 1999. Aerodynamic Design Optimization on Unstructured Grids with a Continuous Adjoint Formulation. Comput. Fluids 28: 443-480.
[32] C. Lozano. 2012. Adjoint Viscous Sensitivity Derivatives with a Reduced Gradient Formulation. AIAA J. 50(1): 203-214.

DOI: 10.13009/EUCASS2019-291

[33] W. Schmidt, A. Jameson and D. Whitfield. 1983. Finite volume solutions to the Euler equations in transonic flow. Journal of Aircraft 20(2): 127-133.
[34] A. Fikl. 2016. Adjoint-Based Optimization for Hyperbolic Balance Laws in the Presence of Discontinuities. M.Sc. Thesis, University of Illinois at Urbana-Champaign.